



## Measurement of one-bond $^{15}\text{N}$ - $^{13}\text{C}'$ dipolar couplings in medium sized proteins

James J. Chou, Frank Delaglio & Ad Bax

Laboratory of Chemical Physics, National Institute of Diabetes and Digestive and Kidney Diseases, National Institutes of Health, Bethesda, MA 20892-0520, U.S.A.

Received 16 June 2000; Accepted 2 August 2000

*Key words:* calmodulin, dipolar coupling, HNCO,  $J(\text{NC}')$ , liquid crystal

### Abstract

A simple and accurate method is described for measurement of  $^1J_{\text{C}'\text{N}}$  splittings in isotopically enriched proteins. The method is of the quantitative  $J$  correlation type, and the  $^1J_{\text{C}'\text{N}}$  splitting is derived from the relative intensity in two 3D TROSY-HNCO spectra with  $^1J_{\text{C}'\text{N}}$  dephasing intervals of  $\sim 1/(2^1J_{\text{C}'\text{N}})$  (reference intensity) and  $\sim 1/^1J_{\text{C}'\text{N}}$  (residual intensity). If the two spectra are recorded under identical conditions and with the same number of scans, the random error in the  $^1J_{\text{C}'\text{N}}$  value extracted in this manner is inversely related to the signal-to-noise (S/N) in the reference spectrum. A S/N of 30:1 in the reference spectrum yields random errors of less than 0.2 Hz in the extracted  $^1J_{\text{C}'\text{N}}$  value. Dipolar couplings obtained from the difference in  $^1J_{\text{C}'\text{N}}$  splitting in the isotropic and liquid crystalline phase for the C-terminal domain of calmodulin are in excellent agreement with its 1.68-Å crystal structure, but agree considerably less with the 2.2-Å structure.

### Introduction

Dipolar couplings provide very useful structural information and can considerably improve the accuracy of structures determined by NMR (Ottiger et al., 1997; Tjandra et al., 1997; Clore et al., 1999; Drohat et al., 1999). Dipolar couplings in a macromolecule can be observed when it has a sufficiently large magnetic susceptibility anisotropy (Bastiaan et al., 1987; Tolman et al., 1995) or when the molecule is dissolved in a liquid crystalline phase of large particles (Tjandra and Bax, 1997). Numerous such media are available to date, ranging from bicelles (Sanders and Schwonek, 1992), filamentous phage (Clore et al., 1998; Hansen et al., 1998), and Helfrich phases (Barrientos et al., 2000; Prosser et al., 1998), to cellulose crystallites (Fleming et al., 2000). Most dipolar coupling measurements have focused on one-bond  $^1\text{H}$ - $^{15}\text{N}$ ,  $^1\text{H}$ - $^{13}\text{C}$ ,  $^{13}\text{C}$ - $^{13}\text{C}$ , and  $^{13}\text{C}$ - $^{15}\text{N}$  couplings, with emphasis on the protein backbone interactions, which in favorable cases contain sufficient information to build an accurate model for the protein (Delaglio et al., 2000).

The present paper concerns the measurement of backbone  $^1D_{\text{C}'\text{N}}$  couplings. Owing to the low magnetogyric ratio of both  $^{13}\text{C}$  and  $^{15}\text{N}$ , and the relatively long internuclear distance (1.33 Å), the  $^1D_{\text{C}'\text{N}}$  dipolar coupling is intrinsically 8.3 times smaller than  $^1D_{\text{NH}}$  (Ottiger and Bax, 1998). Therefore, accuracy of  $^1D_{\text{C}'\text{N}}$  measurement is critical to its utility. Previously,  $^1D_{\text{C}'\text{N}}$  values were obtained from the change in  $^1J_{\text{C}'\text{N}}$  splitting between the isotropic and aligned phase, as measured from the in-phase splitting in  $^{13}\text{C}'$ -coupled HSQC or TROSY spectra (Ottiger and Bax, 1998; Pervushin et al., 1998; Wang et al., 1998) or the antiphase splitting in a  $^{13}\text{C}'$ -coupled TROSY-HNCO spectrum (Kontaxis et al., 2000). A problem in those methods is that many of the  $^{15}\text{N}$ - $\{^{13}\text{C}'\}$  doublets are insufficiently resolved for measuring the splitting at the required high degree of accuracy. Another recent method (Permi and Annala, 2000) solves this problem by separately displaying the two  $^{15}\text{N}$ - $\{^{13}\text{C}'\}$  doublet components in two sub-spectra, in a manner analogous to the previously described in-phase/antiphase (IPAP) and  $S^3\text{E}$  methods (Sørensen et al., 1997; Ottiger et al., 1998), albeit at a significant cost in S/N.

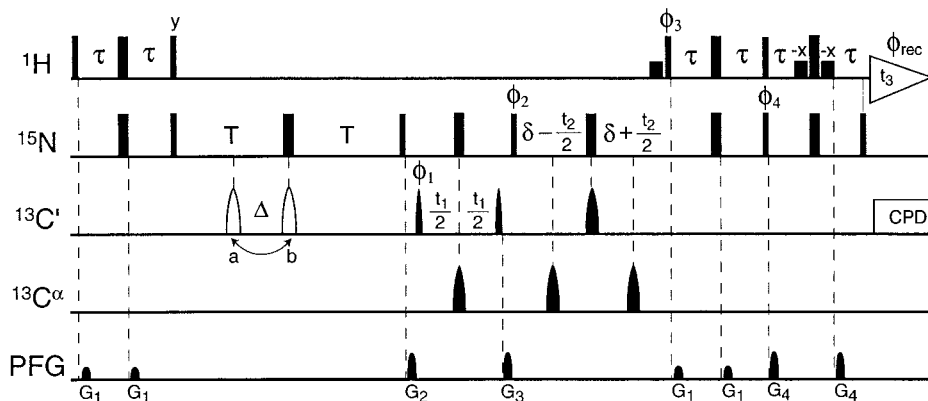


**Figure 1.** Pulse scheme of the 3D TROSY-HNCO quantitative  $J_{C/N}$  experiment. Narrow and wide pulses correspond to flip angles of  $90^\circ$  and  $180^\circ$  respectively. All pulse phases are  $x$ , unless specified otherwise. The  $y$  and  $-y$  phases are interchanged on Varian spectrometers relative to phases reported here for Bruker.  $^{13}\text{C}'$  pulses bracketing the  $t_1$  evolution period are  $90^\circ$  and have the shape of the center lobe of a  $\text{sinc}/x$  function, and durations of  $100 \mu\text{s}$  (at  $200 \text{ MHz } ^{13}\text{C}$  frequency). The other two  $^{13}\text{C}'$  pulses are hyperbolic secant shaped (1 ms) and correspond to  $180^\circ$ . Composite pulse  $^{13}\text{C}'$  decoupling (CPD) was used during acquisition. All three  $^{13}\text{C}'$  pulses are sine-bell shaped and have durations of  $100 \mu\text{s}$ . Delay durations:  $\tau = 2.5 \text{ ms}$ ;  $T = 33.7$ ;  $\delta = 16 \text{ ms}$ ;  $\Delta = 16.6 \text{ ms}$ . For the reference spectrum, the first  $180^\circ$   $^{13}\text{C}'$  pulse (open shape) is applied in position  $a$ ; for the rephased, attenuated spectrum in position  $b$ . Two FIDs are acquired and stored separately for obtaining quadrature selection of the TROSY component in the  $t_2$  dimension, with phases  $\phi_2 = y, x$ ,  $\phi_3 = -y$ ,  $\phi_4 = -y$  and with phases  $\phi_2 = y, -x$ ,  $\phi_3 = y$ ,  $\phi_4 = y$  (Pervushin et al., 1998). In both cases,  $\phi_1 = x, x, -x, -x$ , and Receiver =  $x, y, -x, -y$ . States-TPPI quadrature selection is used in the  $t_1$  dimension. Sine-bell shaped pulsed field gradients (1 ms each) have strength (G/cm) and axis:  $G_1: 3, x$ ;  $G_2: 18, y$ ;  $G_3: 18, x$ ;  $G_4: 18, z$ .

Here we present a conceptually very simple method, which overcomes the problems associated with the accurate measurement of splittings from a poorly resolved doublet. The method is based on the principle of quantitative J correlation (Bax et al., 1994), where the value of the coupling is extracted from the amplitude ratio of two resonances, and not from a difference in resonance frequencies.

## Results and discussion

### Pulse scheme description

Two interleaved TROSY-HNCO spectra need to be recorded with the pulse scheme of Figure 1. In both cases, the  $^{15}\text{N}$ - $\{^{13}\text{C}'\}$  dephasing delay is adjusted to  $2T=66.7 \text{ ms}$ , but in one case (reference spectrum) the  $180^\circ$   $^{15}\text{N}$  and  $^{13}\text{C}'$  pulses are separated by  $\Delta=16.7 \text{ ms}$ , making the effective dephasing time  $2T - 2\Delta=33.3 \text{ ms}$ , i.e., very close to  $1/(2^1J_{C/N})$ . In the second spectrum, the two  $180^\circ$  pulses are coincident and the  $^{15}\text{N}$ - $^{13}\text{C}'$  coupling remains active for the entire interval. The  $^{15}\text{N}$ - $\{^{13}\text{C}'\}$  doublet components are nearly rephased at the end of the  $2T$  period, yielding resonances with very weak residual intensity, proportional to:

$$I_{\text{att}} = A \sin(2\pi^1J_{C/N}T), \quad (1a)$$

where  $A$  is a constant which depends on the number of scans, sample concentration, etc. For the reference spectrum, the corresponding resonance intensity is

$$I_{\text{ref}} = A \sin[2\pi^1J_{C/N}(T - \Delta)]. \quad (1b)$$

The value of  $^1J_{C/N}$  is then extracted from the  $I_{\text{att}}/I_{\text{ref}}$  ratio, either by a simple one-dimensional grid search, or by a non-linear fit.

One point that requires special attention is the correct measurement of  $I_{\text{att}}$ . Many resonances in the rephased, attenuated spectrum have near zero intensity and regular peak picking would yield amplitudes with an absolute value that is at least as large as the rms noise in the spectrum. Instead, we determine the interpolated peak position from the high sensitivity reference spectrum, and measure the  $I_{\text{att}}$  intensity in the attenuated spectrum at exactly the same position, using the 3D Fourier interpolation feature in NMRPipe (Delaglio et al., 1995).

The method is applicable to any protein which yields high S/N ( $\geq 20:1$ ) HNCO spectra in a reasonable amount of time. By using the TROSY version of the HNCO experiment (Salzmann et al., 1999), even relatively large proteins can be studied in this manner.

### Data collection

The method is demonstrated for a sample of protonated,  $\text{U-}^{13}\text{C}/^{15}\text{N}$  ( $>98\%$ )  $\text{Ca}^{2+}$ -mammalian calmod-

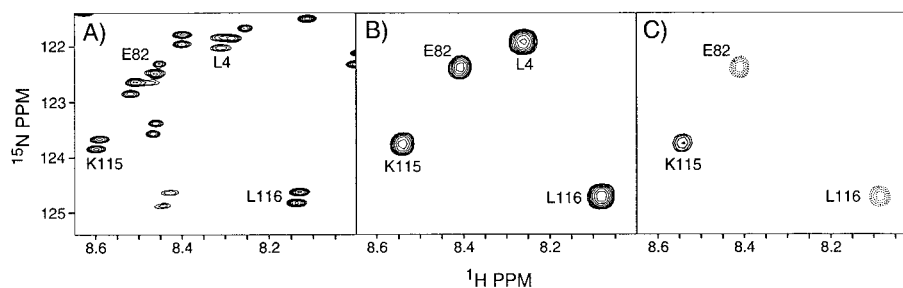


Figure 2. Small  $^1\text{H}$ - $^{15}\text{N}$  regions (800 MHz) taken from (A) the downfield  $^{15}\text{N}$ - $\{^1\text{H}\}$  doublet component of the  $^{13}\text{C}'$ -coupled IPAP-HSQC spectrum, (B) the reference TROSY-HNCO spectrum, and (C) the rephased, attenuated TROSY-HNCO spectrum of CaM in the  $\text{Ca}^{2+}$  ligated form in the presence of 180 mg/ml Pf1. Positive intensity indicates  $J_{\text{C}'\text{N}} + D_{\text{C}'\text{N}} < (2T)^{-1}$ ; negative intensity (dashed contours) indicates  $J_{\text{C}'\text{N}} + D_{\text{C}'\text{N}} > (2T)^{-1}$ ; below-threshold intensity for L4 in (C) indicates a  $J_{\text{C}'\text{N}} + D_{\text{C}'\text{N}}$  value close to the null condition,  $(2T)^{-1} = 15.0$  Hz.

ulin (CaM; 148 residues, 16.7 kDa).  $^1J_{\text{C}'\text{N}}$  splittings are measured for an isotropic sample, containing 5 mg CaM in 300  $\mu\text{l}$  95%  $\text{H}_2\text{O}$ , 5%  $\text{D}_2\text{O}$  (1 mM), pH 7.0, 100 mM NaCl, and for a second sample containing an additional 18 mg/ml of the filamentous phage Pf1 (Hansen et al., 1998) (Asla Labs, <http://130.237.129.141//asla/asla-phage.htm>). Spectra were recorded at 25  $^\circ\text{C}$  and 800 MHz  $^1\text{H}$  frequency. The high field enhances the TROSY effect and causes a slight decrease in transverse  $^{15}\text{N}$  relaxation rate relative to 600 MHz, but was used primarily to permit comparison with the regular  $^{13}\text{C}'$ -coupled IPAP-HSQC spectrum (Wang et al., 1998) which exhibits extensive overlap at 600 MHz. The two interleaved TROSY-HNCO spectra were recorded with the pulse scheme of Figure 1. Each spectrum was acquired as a  $32^* \times 60^* \times 512^*$  data matrix with acquisition times of 16 ms ( $t_1$ ,  $^{13}\text{C}'$ ), 30 ms ( $t_2$ ,  $^{15}\text{N}$ ), and 102 ms ( $t_3$ ,  $^1\text{H}$ ), using 16 scans per hypercomplex ( $t_1, t_2$ ) increment (4 scans per FID), and a total measuring time of 20 h for the pair of interleaved spectra. Data were processed and analyzed using NMRPipe.

#### Application to $\text{Ca}^{2+}$ -calmodulin

Figure 2 compares a small region of the downfield  $^{15}\text{N}$ - $\{^1\text{H}\}$  doublet component of the  $^{13}\text{C}'$ -coupled 2D IPAP-HSQC spectrum, recorded in the Pf1 medium, with two cross sections through the reference and attenuated 3D TROSY-HNCO spectra, taken at a  $^{13}\text{C}'$  frequency of 175.6 ppm. As can be seen from this figure, considerable overlap is present in the 2D IPAP-HSQC spectrum, even at 800 MHz. Moreover, several of the  $^{15}\text{N}$ - $\{^{13}\text{C}'\}$  doublets are insufficiently resolved for accurate measurement of the  $^1J_{\text{C}'\text{N}}$  splitting. From the IPAP-HSQC spectrum, 42 out of a total possible 67  $^1J_{\text{C}'\text{N}}$  couplings could be measured for the C-terminal

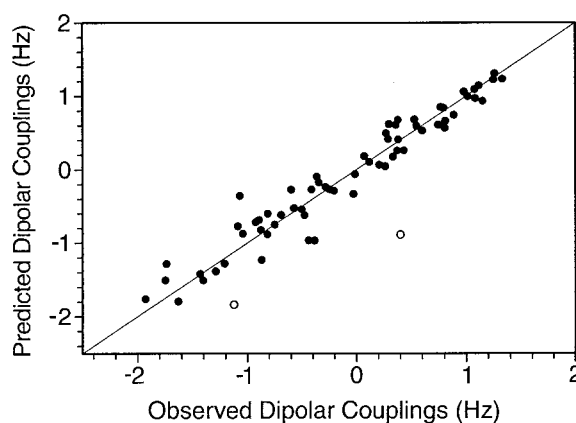


Figure 3. Correlation between observed  $D_{\text{C}'\text{N}}$  values, and values predicted for the C-terminal CaM domain (PDB entry 1OSA) using an alignment tensor obtained from best fitting  $D_{\text{C}'\text{N}}$  values to the crystal structure. The correlation coefficient,  $R$ , equals 0.969. Open circles correspond to the two C-terminal peptide bonds and are not included in the fit.

domain of CaM (residues E82-K148). In contrast, all 67 cross peaks in the 3D HNCO spectrum are free of overlap and permitted measurement of the corresponding  $^1D_{\text{C}'\text{N}}$  dipolar couplings. A best fit, calculated using the SVD method (Losonczi et al., 1999) incorporated in the program SSIA (Zweckstetter and Bax, 2000), between the  $^1D_{\text{C}'\text{N}}$  dipolar couplings and CaM C-terminal domain X-ray structure (Ban et al., 1994) (PDB entry 1OSA) is shown in Figure 3. The correlation coefficient,  $R$ , equals 0.97 and the rms difference between measured and predicted dipolar couplings is 0.21 Hz. Comparison of the measured  $^1J_{\text{C}'\text{N}}$  splittings with the values derived from the 2D spectrum of Figure 2A indicates that systematic errors in the new approach are negligible (data not shown).

The 0.21 Hz rmsd includes the errors in the measured couplings (0.14 Hz, see *Error analysis*), and

contributions from the uncertainty in the coordinates of the X-ray structure, non-uniform scaling as a result of varying degrees of internal dynamics along the polypeptide backbone, and small differences between the average structure in solution and in the crystalline state. When comparing measured  $^1D_{C'N}$  data with the original, 2.2-Å mammalian CaM X-ray structure (Babu et al., 1988) (PDB entry 3CLN), the correlation is considerably poorer ( $R = 0.85$ ), with a rmsd of 0.45 Hz between measured and best-fitted  $^1D_{C'N}$  values (data not shown).

### Error analysis

The estimated random error in the splitting extracted using Equation 1 is dominated by the random noise in the attenuated spectrum. The derivative of  $I_{att}$  with respect to  $J$  equals:

$$dI_{att}/dJ = 2A\pi T \cos(2\pi JT) \approx -2A\pi T \quad (2)$$

The resonance intensity in the reference spectrum is approximately equal to  $A$ , because  $\sin[2\pi^1J_{C'N}(T - \Delta)] \approx 1$ . If the rms noise is  $\sigma$ , the error in the  $J$  splitting derived from Equation 1 therefore equals  $\sigma/(2\pi AT)$ . This number only serves to give an indication of the approximate accuracy of the random error in the extracted  $J$  coupling. When the condition  $2JT = 1$  is not fulfilled, the effect of the random error in the reference spectrum increases, and simulated data with added random noise confirm that the error in the extracted  $J$  becomes larger than  $\sigma/(2\pi AT)$ , although not by much provided the true splitting does not deviate by more than  $\sim 2.5$  Hz from the selected target value (15 Hz;  $2T=66.7$  ms). The average S/N in the reference TROSY-HNCO spectrum was ca. 50:1, indicating a random error in the measured  $J$  splittings of 0.1 Hz, and a random error of  $0.1\sqrt{2} \approx 0.14$  Hz in the extracted dipolar coupling.

It is also interesting to consider the effect of long range couplings on the derived  $^1J_{C'N}$  value. Except for couplings between  $^{15}N$  and carbons resonating in the  $^{13}C'$  region, all these couplings attenuate the reference and attenuated spectrum by the same factor, and therefore do not affect the derived coupling. The presence of through-hydrogen-bond  $^3J_{C'N}$  coupling (Cordier and Grzesiek, 1999), intraresidue  $^2J_{C'N}$  coupling, and intraresidue  $^3J_{C'N}$  coupling in Asn and Asp residues affects the reference and attenuated spectra differentially, however. Both  $^3J_{C'N}$  and  $^2J_{C'N}$  have absolute values of at most ca. 1 Hz (Cornilescu et al., 1999), whereas trans  $^3J_{C'N}$  couplings in Asp and Asn can be

as large as 2.5 Hz. A passive 2.5 Hz coupling attenuates the reference intensity by 3.4%, and the attenuated signal by 13.4%, so it decreases the  $I_{att}/I_{ref}$  ratio by 10%, resulting in a coupling that is 10% closer to 15 Hz than its real value. So, a true coupling of 13 Hz would appear as a 13.2 Hz coupling, and a 17 Hz coupling would appear to be 16.8 Hz. The effect of the systematic error introduced in this manner scales with the square of the passive coupling. Long-range  $D_{C'N}$  couplings are negligible under normal experimental conditions ( $<0.5$  Hz). If we assume a 1.2-Hz upper limit for the passive coupling in non-Asx residues, this results in a maximum error of 0.05 Hz, which typically is considerably smaller than the random error.

### Concluding remarks

The approach described here provides a simple and sensitive alternative to the measurement of  $^1J_{C'N}$  by E.COSY methods. The difference in  $^1J_{C'N}$  splitting between isotropic and aligned states yields the  $^1D_{C'N}$  coupling, which is proving to be very useful in structure determination. The value of the isotropic  $^1J_{C'N}$  splitting has been shown to be related to hydrogen bond strength (Juranic et al., 1995), which provides another interesting use for its measurement.

It is also possible to conduct the measurement of  $^1D_{C'N}$  in a 2D manner, but using the same principle. One way to do this simply leaves  $t_1$  ( $^{13}C'$ ) in Figure 1 fixed at 0 (also removing the  $^{15}N$  and  $^{13}C'$   $180^\circ$  pulses applied during  $t_1$ ), and possibly uses a mixed-constant time  $^{15}N$  evolution period (Grzesiek and Bax, 1993; Logan et al., 1993) to increase resolution in the  $^{15}N$  dimension of the 2D spectrum.

A second, even simpler and somewhat more sensitive method records two regular constant-time (CT = 100 ms) TROSY  $^{15}N$ - $^1H$  spectra, either with the  $^{13}C'$  decoupled (reference spectrum) or with the  $^{13}C'$   $180^\circ$  decoupling pulse applied simultaneously to the moving  $180^\circ$   $^{15}N$  pulse. It should be noted, however, that this latter approach is sensitive to incomplete  $^{13}C$  enrichment, which can result in systematically altered  $^1J_{C'N}$  splittings. Also, because the constant time is preferentially set to 100 ms in this experiment, the systematic error introduced by the effect of passive couplings (see *Error analysis*) is not necessarily negligible. Because the 3D approach yields less resonance overlap, resulting in a virtually complete set of  $^1D_{C'N}$  values, we generally prefer to record the spectra in the 3D mode.

Interleaved 3D TROSY-HNCO and 2D CT-TROSY pulse schemes, coded for Bruker DRX spectrometers, can be found at <http://spin.niddk.nih.gov/bax>.

## References

- Babu, Y.S., Bugg, C.E. and Cook, W.J. (1988) *J. Mol. Biol.*, **204**, 191–204.
- Ban, C., Ramakrishnan, B., Ling, K.Y., Kung, C. and Sundaralingam, M. (1994) *Acta Crystallogr.*, **D50**, 50–63.
- Barrientos, L.G., Dolan, C. and Gronenborn, A.M. (2000) *J. Biomol. NMR*, **16**, 329–337.
- Bastiaan, E.W., Maclean, C., van Zijl, P.C.M. and Bothner-By, A.A. (1987) *Annu. Rep. NMR Spectrosc.*, **19**, 35–77.
- Bax, A., Vuister, G.W., Grzesiek, S., Delaglio, F., Wang, A.C., Tschudin, R. and Zhu, G. (1994) *Methods Enzymol.*, **239**, 79–105.
- Clore, G.M., Starich, M.R., Bewley, C.A., Cai, M.L. and Kuszewski, J. (1999) *J. Am. Chem. Soc.*, **121**, 6513–6514.
- Clore, G.M., Starich, M.R. and Gronenborn, A.M. (1998) *J. Am. Chem. Soc.*, **120**, 10571–10572.
- Cordier, F. and Grzesiek, S. (1999) *J. Am. Chem. Soc.*, **121**, 1601–1602.
- Cornilescu, G., Ramirez, B.E., Frank, M.K., Clore, G.M., Gronenborn, A.M. and Bax, A. (1999) *J. Am. Chem. Soc.*, **121**, 6275–6279.
- Delaglio, F., Grzesiek, S., Vuister, G.W., Zhu, G., Pfeifer, J. and Bax, A. (1995) *J. Biomol. NMR*, **6**, 277–293.
- Delaglio, F., Kontaxis, G. and Bax, A. (2000) *J. Am. Chem. Soc.*, **122**, 2142–2143.
- Drohat, A.C., Tjandra, N., Baldisseri, D.M. and Weber, D.J. (1999) *Protein Sci.*, **8**, 800–809.
- Fleming, K., Gray, D., Prasannan, S. and Matthews, S. (2000) *J. Am. Chem. Soc.*, **122**, 5224–5225.
- Grzesiek, S. and Bax, A. (1993) *J. Biomol. NMR*, **3**, 185–204.
- Hansen, M.R., Mueller, L. and Pardi, A. (1998) *Nat. Struct. Biol.*, **5**, 1065–1074.
- Juranic, N., Ilich, P.K. and Macura, S. (1995) *J. Am. Chem. Soc.*, **117**, 405–410.
- Kontaxis, G., Clore, G.M. and Bax, A. (2000) *J. Magn. Reson.*, **143**, 184–196.
- Logan, T.M., Olejniczak, E.T., Xu, R.X. and Fesik, S.W. (1993) *J. Biomol. NMR*, **3**, 225–231.
- Losonczi, J.A., Andrec, M., Fischer, M.W.F. and Prestegard, J.H. (1999) *J. Magn. Reson.*, **138**, 334–342.
- Ottiger, M. and Bax, A. (1998) *J. Am. Chem. Soc.*, **120**, 12334–12341.
- Ottiger, M., Delaglio, F. and Bax, A. (1998) *J. Magn. Reson.*, **131**, 373–378.
- Ottiger, M., Tjandra, N. and Bax, A. (1997) *J. Am. Chem. Soc.*, **119**, 9825–9830.
- Permi, P. and Annala, A. (2000) *J. Biomol. NMR*, **16**, 221–227.
- Pervushin, K.V., Wider, G. and Wüthrich, K. (1998) *J. Biomol. NMR*, **12**, 345–348.
- Prosser, R.S., Losonczi, J.A. and Shiyonovskaya, I.V. (1998) *J. Am. Chem. Soc.*, **120**, 11010–11011.
- Salzmann, M., Wider, G., Pervushin, K., Senn, H. and Wüthrich, K. (1999) *J. Am. Chem. Soc.*, **121**, 844–848.
- Sanders, C.R. and Schwonek, J.P. (1992) *Biochemistry*, **31**, 8898–8905.
- Sørensen, M.D., Meissner, A. and Sørensen, O.W. (1997) *J. Biomol. NMR*, **10**, 181–186.
- Tjandra, N. and Bax, A. (1997) *Science*, **278**, 1111–1114.
- Tjandra, N., Omichinski, J.G., Gronenborn, A.M., Clore, G.M. and Bax, A. (1997) *Nat. Struct. Biol.*, **4**, 732–738.
- Tolman, J.R., Flanagan, J.M., Kennedy, M.A. and Prestegard, J.H. (1995) *Proc. Natl. Acad. Sci. USA*, **92**, 9279–9283.
- Wang, Y.X., Marquardt, J.L., Wingfield, P., Stahl, S.J., Lee-Huang, S., Torchia, D. and Bax, A. (1998) *J. Am. Chem. Soc.*, **120**, 7385–7386.
- Zweckstetter, M. and Bax, A. (2000) *J. Am. Chem. Soc.*, **122**, 3791–3792.